Apoptosis (2009) 14:203–217
DOI 10.1007/s10495-008-0291-9

ORIGINAL PAPER

Sodium butyrate sensitizes human colon adenocarcinoma COLO 205 cells to both intrinsic and TNF-α-dependent extrinsic apoptosis

Beata Pajak · Barbara Gajkowska · Arkadiusz Orzechowski

Published online: 7 January 2009
© Springer Science+Business Media, LLC 2009

Abstract Overexpression of cFLIP protein seems to be critical in the antiapoptotic mechanism of immune escape of human COLO 205 colon adenocarcinoma cells. Actually, cFLIP appears to inhibit the death receptor ligand-mediated cell death. Application of the metabolic inhibitor sodium butyrate (NaBt), short-chain volatile fatty acid, sensitized COLO 205 cells to TNF-α-mediated apoptosis. Western-blot analysis revealed that the susceptibility of human COLO 205 cells to apoptogenic stimuli resulted from time-dependent reduction in cFLIP and simultaneous up-regulation of TNF-R1 protein levels. Additionally, the combined TNF-α and NaBt treatment caused cleavage of Bid and caspase-9 activation, as well as cytochrome *c* release from mitochondria. Thus, the evidence of this study indicates that NaBt facilitates the death receptor signal evoked by TNF-α. Moreover, NaBt alone initiated intrinsic apoptosis, that in turn was abolished by intracellular BCL-2 delivery. It confirms the involvement of mitochondria in the proapoptotic activity of NaBt. The activation of mitochondrial pathway was substantiated by up-regulated expression of BAK with concomitant reduction of antiapoptotic BCL-x_L, XIAP and survivin proteins. These findings suggest that NaBt could represent a good candidate for the new therapeutic strategy aimed to improve chemo- and immunotherapy of colon cancer.

B. Pajak (✉) · B. Gajkowska · A. Orzechowski
Department of Cell Ultrastructure, Mossakowski Medical Research Center, Polish Academy of Sciences, Pawinskiego 5, 02-106 Warsaw, Poland
e-mail: bepaj@wp.pl

A. Orzechowski
Department of Physiological Sciences, Faculty of Veterinary Medicine, Warsaw University of Life Sciences (SGGW), Nowoursynowska 159, 02-776 Warsaw, Poland

Keywords TNF-α · Sodium butyrate · cFLIP · Intrinsic apoptosis · Immune escape · Colon cancer

Introduction

Resistance or failure to undergo apoptosis is an integral attribute of colorectal tumor cells [1]. Better understanding of this phenomenon would be helpful at restoration of normal cellular response or to increase the susceptibility to apoptosis. An optimal anti-tumor drug would be one which selectively induces apoptosis in cancer but not in the normal cells. There is increasing evidence from in vitro and in vivo studies [2–5] that short chain fatty acid (SCFA) butyrate, naturally produced during microbial fermentation of dietary fiber in the colon [6], is a promising factor with such properties.

It has been long established that SCFA play an important role in homeostasis of the colonic mucosa by inducing pathways of cell maturation, including cell cycle arrest, differentiation and apoptosis [7]. In human colorectal cancer, sodium butyrate has been shown to inhibit proliferation and to exert potent anticancer effect on transformed colonocytes by apoptosis induction (for details see the review by Pajak et al. [8]). Numerous data suggest that sodium butyrate most likely acts through inhibition of histone deacetylase, thus leading to hyperacetylation of chromatin components such as histones and non-histone proteins, and finally to alternations in various pro- or/and antiapoptotic gene expression [9, 10].

Apoptosis is a cell death process which is transmitted by two major pathways, namely the extrinsic and the intrinsic apoptotic pathway. The extrinsic pathway is activated via death receptors and utilizes protein interaction modules known as death domains (DDs) and death effector domains (DEDs) to assemble signaling complexes that induce

apoptosis [11]. TNF-R1 is a member of the death receptor family, whose binding with its natural ligand, TNF-α activates extrinsic pathway of apoptosis in TNF-R1 expressing cells [12]. Among the proteins which have been identified as inhibiting extrinsic apoptosis, the cellular FLICE-like inhibitory protein (cFLIP) seems to play considerable role. cFLIP structurally resembles caspase-8 but it lacks proteolytic activity, thus it functions as a dominant negative inhibitor of caspase-8 (FLICE) [12]. A critical role of cFLIP in the resistance of certain cancers to death ligands has been demonstrated by several authors [13–15] with a reduction in cellular levels of cFLIP to assist elevated sensitivity of cancers to death ligands.

The intrinsic pathway of apoptosis, that involves mitochondria and the release of caspase-activating proteins, is regulated mainly by two groups of apoptosis-related proteins, BCL-2 and IAP families. BCL-2 family of proteins includes both antiapoptotic (BCL-2, BCL-x_L) and proapoptotic (BAK, BAD, BAX, BID, BIM, BCL-x_S) members which share structural homologies and can physically interact with each other to form homo- or hetero-dimers [16]. Contradictory, IAP proteins, such as NAIP, cIAP1, cIAP2, XIAP and survivin, all are suppressors of apoptosis regardless of type of stimulus [17]. Importantly, the balance of antiapoptotic and proapoptotic proteins determines, in part, how cells react to apoptotic signal. Cancer cells are usually resistant to both apoptotic pathways.

In the present study, we investigated the effect of NaBt treatment on cell viability and apoptosis of colon adenocarcinoma COLO 205 cells. Our results demonstrate that NaBt is able to potentiate either of apoptotic pathways. Moreover, we found that decrease in cFLIP expression represents an important molecular mechanism of NaBt-mediated sensitization of colon cancer cells to TNF-α-induced apoptosis. In addition, the TNF-R1-mediated cell death was further amplified by activation of intrinsic apoptotic pathway. Furthermore, higher doses of NaBt evoked the intrinsic apoptosis, irrespective to TNF-α. The activation of mitochondrial pathway resulted from NaBt-mediated modulation of BCL-x_L, BAK, XIAP and survivin proteins. These features are indicative for the advanced colon cancer. Additionally, at this stage tumor is refractory to almost all known therapies. The potency of NaBt suggests that this SCFA could be considered seriously as a starting material to develop a new strategy in cancer therapy.

Materials and methods

Reagents

All reagents: dimethyl sulfoxide (DMSO), Tris, 4-(2-hydroxyethyl)-1-piperazine-ethanesulfonic acid (HEPES), ethylenediaminetetraacetic acid (EDTA), (2-aminoethoxyethane)-*N*,*N*,*N*′,*N*′-tetraacetic acid (EGTA), polyoxyethylene sorbitan monolaurate (TWEEN 20), sodium chloride (NaCl), bovine serum albumin (BSA), 3-(4,5-dimethylthiazol-2-yl)-2-5-diphenyltetrazolium bromide (MTT), phenylmethylsulphonylfluoride (PMSF), dithiothreitol (DTT), paraformaldehyde, cycloheximide (CHX), actinomycin D (AD), bisbenzimide (HO33342), propidium iodide (PI), tumor necrosis factor-α (TNF-α), sodium butyrate (NaBt), z-Ile-Glu(O-Me)-Thr-Asp(O-Me) fluoromethyl ketone (z-IETD-fmk), D-mannitol, sucrose, Igepal CA-630 were cell culture tested, of high purity, and unless otherwise stated purchased from Sigma–Aldrich Chemical Co. (St. Louis, MO, USA). *N*-Benzyloxycarbonyl-Val-Ala-Asp(O-Me) fluoromethyl ketone (z-VAD-fmk) was purchased from Calbiochem (San Diego, CA, USA). Reagents for experimental use were prepared according to the manufacturer's recommendations and if possible stored as stock solutions (1,000-fold the highest working concentration). All primary and secondary horseradish peroxidase (HRP) conjugated antibodies were obtained from Santa Cruz Biotechnology (Santa Cruz, CA, USA). Other reagents were purchased as stated in the description of the respective methods (see the text). Sodium dodecyl sulfate (SDS) 100 g/l, sequi-blot polyvinylidene fluoride (PVDF) membrane 0.2 μm and all reagents for immunoblotting were obtained from Bio-Rad Laboratories (Hercules, CA, USA). Sera, media and antibiotics were obtained from Gibco Life Technologies (Paisley, United Kingdom).

Cell culture

Human colon adenocarcinoma cell line COLO 205 was purchased from American Type Culture Collection (ATCC). Cells were maintained in the exponential phase of growth in growth medium [GM, 100 ml/l Fetal Bovine Serum (FBS)/Dulbecco's Modified Eagle Medium (DMEM) with Glutamax and antibiotic–antimycotic mixture (Penicillin G sodium salt 50 IU/ml, Streptomycin sulfate 50 μg/ml, Gentamycin sulfate 20 μg/ml, Fungizone–Amphotericin B 1 μg/ml)]. The cells were grown at 37°C, in a controlled, humidified 50 ml/l CO_2 atmosphere, on 96-well flat-bottomed or tissue culture Petri dishes (100 mm diameter, BD Biosciences Pharmingen, San Jose, CA, USA).

Experimental procedure

During propagation, the medium was changed every other day until cultures reached 100% confluence. One-day (24 h) prior to the experiment, confluent cells (cells of the same cell density fully covering the surface of the dish) were then switched to post-mitotic status to induce quiescence (withdrawal from cell cycle) by replacing GM with

20 g/l BSA/DMEM designated as a control medium (CTRL). In the above-mentioned conditions divisions of COLO 205 cell have been completed. During the study freshly prepared media with or without experimental factors had been changed according to the experimental schedule.

Cell viability

Cell viability based on mitochondrial function was assayed by the ability of cells to convert soluble MTT (3-(4,5-dimethylthiazol-2-yl)-2-5-diphenyltetrazolium bromide) into an insoluble purple formazan reaction product with minor modifications to protocol described by Jacobson [18]. For this assay, during the last hour of incubation the media were replaced with MTT solution (5 mg/ml in DMEM without phenol red, sterilized by filtration). MTT solution was then aspirated and formazan in cells was instantly dissolved by the addition of 100 µl DMSO. Before the application of MTT, cells were examined under phase-contrast microscopy to visually assess the degree of cell death. The absorbance was measured at 570 nm with ELISA reader type Infinite 200 (TECAN, Austria). Percentage of viable cells was measured by MTT conversion into purple formazan either in 20 g/l BSA/DMEM or 1 ml/l DMSO and was related to mitochondrial respiration or activity of mitochondrial dehydrogenases.

Apoptotic index and detection of apoptotic cells using morphological criteria

Cells were grown on Lab-Tek 4-Chamber Slide w/Cover (Permanox Slide Sterile, Nalge Nunc International, Naperville, IL, USA). Cytotoxicity with resultant cell death was evaluated by microscopic observations. Apoptosis was evaluated by in situ uptake of propidium iodide (PI) and bisbenzimide (HO33342) as described by McKeague et al. [19]. To avoid detachment the cells were then washed gently with medium. Attached cells were stained by both propidium iodide followed by Hoechst 33342 staining to distinguish live, necrotic, early- and late-apoptotic cells. Afterwards, the cells were fixed with an equal volume of methanol/acetic acid (3:1, v/v) and the cells were gently washed with ice cold PBS (Phosphate-Buffered Saline including Ca^{2+} and Mg^{2+}) and mounted on slides using mounting medium prepared according to the manufacturer's protocol (Mowiol, CN Biosciences Inc., La Jolla, CA, USA). A BX-60 Olympus fluorescent microscope equipped with a PM20 automatic photomicrograph system was used for photographic recording. At least one hundred nuclei were counted under ultraviolet light in ten (or more if necessary) randomly chosen visual fields per slide. In the same visual field the excitation of propidium iodide should lead to the appearance of red nuclei of the necrotic dead cells (no such cells have been detected). Cells were considered apoptotic if they were PI-negative and chromatin was condensed at the periphery of nuclei. Apoptotic index was calculated from the number of apoptotic nuclei versus total number of nuclei at each visual field ($n = 10$). Three independent experiments were performed.

Ultrastructural studies

Cells were fixed in 2% paraformaldehyde and 2.5% glutaraldehyde in 0.1 M sodium cacodylate buffer (pH 7.4) for 2 h at 4°C. Cells were washed with the same buffer and post-fixed with 1% OsO_4 in 0.1 M sodium cacodylate buffer for 1 h. Next, cells were dehydrated in a graded ethanol:water solutions and embedded in Epon 812. Ultrathin sections were mounted on the formvar-coated copper grids, air-dried and stained for 10 min with 4.7% uranyl acetate and for 2 min with lead citrate. The sections were examined and photographed with a JEOL 1011XE electron microscope (Jeol, Tokyo, Japan).

Quantitative apoptotic cell death assay

To quantify TNF-α [10 ng/ml] or NaBt [2 mM, 5 mM]- or TNF-α [10 ng/ml] + NaBt [2 mM]-induced apoptotic death of COLO 205 cells, Annexin V and PI staining were performed followed by FCM (BD Biosciences Pharmingen, San Jose, CA, USA). COLO 205 cells grown in log phase were plated onto 6-well plates and allowed to attach in GM for 24 h. This was followed by one-day pretreatment with CTRL medium. Finally, the medium was replaced with an equal volume of fresh CTRL medium containing different concentrations [2, 5 mM] of NaBt or TNF-α [10 ng/ml] or TNF-α + NaBt [2 mM] or TNF-α + NaBt [2 mM] + z-IETD-fmk [20 µM] or NaBt [5 mM] + z-VAD-fmk [10 µM] for desired period of time (4 h). After the treatment period, the cells were detached by trypsinization, trypsin was inactivated and cells were washed twice with PBS. A volume of 100 µl of cell suspension was subjected to 5 µl Annexin V and 10 µl of PI staining and then cells were left in the dark for 15 min. Next, 400 µl of cold binding buffer was added and cells were mildly vortexed and tubes with cells were transferred on ice. Cytometric data were collected using a FACSvantage flow cytometer and analyzed by CellQuest software (BD Biosciences, San Jose, CA, USA).

Cells subfractionation and detection of cytochrome *c*

Cells were washed once with ice-cold PBS, scraped, and then resuspended in 500 µl ice-cold HIM buffer (200 mM D-mannitol, 70 mM sucrose, 10 mM HEPES, 1 mM EGTA,

pH 7.4) supplemented with 0.4 mM PMSF, 10 μg/ml of aprotinin, 1 mM DTT and 10 μg/ml of sodium orthovanadate. Cells were incubated on ice for 15 min and then passed through a gauge #25 (25G) needle 20 times to disrupt cell membranes. The cell homogenates were applied to a series of centrifugations. First, cell nuclei were spun down at 1,000*g* for 10 min and 4°C followed by centrifugation of supernatant at 9,000*g* for 20 min, 4°C to isolate mitochondrial fraction. After the final centrifugation the supernatant was collected as the cytosolic fraction. Protein concentration in the cytoplasmic fraction was determined by a protein-dye-binding method [20] with a commercial reagent (Bio-Rad Laboratories, Hercules, CA, USA). The equal amounts of cytosolic fraction were subjected to 12% SDS/PAGE analysis to evaluate the level of cytochrome *c*.

Isolation of cytoplasmic and nuclear fractions

Cells were grown on 100 mm diameter culture Petri dishes. Following each experiment cells were washed twice with PBS, scraped off in PBS and spun down (10,000*g* for 5 min, 4°C). Cell pellets were stored at −80°C until the end of the experiment. Cell pellets were resuspended in 400 μl of ice-cold buffer (10 mM HEPES pH 7.9, 10 mM KCl, 0.1 mM EDTA, 0.1 mM EGTA, 1 mM DTT, 0.5 mM PMSF), then were incubated on ice for 15 min, after which 25 μl of a 100 ml/l solution of Igepal CA-630 was added. After centrifugation (RT, 1,000*g*, 30 s), supernatants containing cytoplasm were transferred to fresh tubes and were stored at −20°C. Nuclear pellets were resuspended in 200 μl RIPA buffer (1× PBS, 10 ml/l Igepal CA-630, 5 g/l sodium deoxycholate, 1 g/l SDS, 0.4 mM PMSF, 10 μg/ml of aprotinin and 10 μg/ml of sodium orthovanadate) and were passed through a 21-gauge needle. After centrifugation (10,000*g* for 5 min, 4°C) nuclear lysates were stored at −80°C until analysis. Soluble protein concentration in the lysate was determined by a protein-dye-binding method [20] with a commercial reagent (Bio-Rad Laboratories, Hercules, CA, USA).

Sample preparation for electrophoresis and immunoblotting

To obtain whole-cell lysates an aliquot of 1 ml of ice-cold PBS was added and cells were immediately scraped from the plastics and collected by centrifugation (10,000*g* for 10 min, 4°C). An aliquot of 1.0 ml of RIPA buffer was added to suspend the cells, which were further broken up by repetitive triturating with the syringe with attached needle (21G, 0.8 mm diameter). Cell lysates were left on ice (4°C) for 30 min, and centrifuged for another 5 min (4°C, 10,000 *g*). The resulting viscous solution was divided into smaller volumes and transferred to fresh Eppendorf tubes and stored at −80°C until used. Soluble protein concentration in the lysates was determined by a protein-dye-binding method [20] with a commercial reagent (Bio-Rad Laboratories, Hercules, CA, USA).

Electrophoresis and immunoblotting

Equal amounts of sample protein (either 50 or 30 μg) isolated from the treated or untreated COLO 205 cells were then resolved by sodium dodecyl sulfate-polyacrylamide gel electrophoresis (SDS–PAGE) followed by immunoblotting. The electrotransfer of proteins to PVDF membranes (0.2 μm) was performed for 1.5 h at 100 V and followed by overnight blocking (4°C) in TBS buffer (20 mM Tris, 500 mM NaCl, pH 7.5) supplemented with 50 g/l non-fat powdered milk. After washing in TBST (TBS containing 0.5 ml/l Tween 20), the membranes were immunostained by standard method provided by the manufacturer (Santa Cruz, CA, USA). They were probed with a primary antibody (mouse monoclonal anti-cFLIP, anti-TNF-R1, anti-procaspase-8, anti-BAX, rabbit polyclonal anti-FADD, anti-procaspase-3, anti-BCL-2, anti-cytochrome *c*, anti-TRAF2, anti-cIAP-1, anti-BCL-x_L, anti-BAK, anti-survivin and goat polyclonal anti-TRADD, anti-BID, anti-caspase-9, anti-RIP, anti-BCL-2, anti-XIAP, anti-PCNA antiserum) (Santa Cruz, CA, USA) for 1 h at 20°C or overnight at 4°C, washed three times in TBST and were further incubated with the secondary donkey anti-rabbit or anti-goat or anti-mouse antibody conjugated with HRP (see "Reagent's" section). Membranes were also probed with goat polyclonal anti-actin (for whole-cell or cytoplasmic lysates) or anti-PCNA (for nuclear lysates) antibody to normalize protein levels. The blots were developed using the enhanced chemiluminescence (ECL) detection system (Amersham International, Aylesbury, UK) according to the manufacturer's protocol. After exposure, photographs were taken with a Kodak DC 290 zoom digital camera and were scanned and analyzed using the Kodak EDAS 290/Kodak 1D 3.5 system.

Immunoprecipitation and western-blotting

Whole-cell lysates containing 900 μg of protein were precleared by adding 0.25 μg of the appropriate control IgG (corresponding to the host species of the primary antibody) together with 20 μl of agarose conjugate (A/G bead slurry; Santa Cruz Biotechnology, Santa Cruz, CA, USA). Cell lysates were incubated at 4°C for 30 min. Afterwards, the beads were spun down at 1,000*g* for 30 s at 4°C. To the cell lysate 1.5 μg (7.5 μl) rabbit polyclonal anti-FADD antibody was added for 2 h at 4°C. Next, 20 μl of agarose conjugate was added and incubation was continued overnight at 4°C. Beads were then washed four

times with ice-cold RIPA buffer, boiled in sample buffer (2× Laemmli buffer) for 2–3 min, separated by 10% SDS–PAGE, transferred to a PVDF membrane and probed with a mouse monoclonal anti-FLIP IgG antibody [1 μg/ml] for detection of endogenous protein associations. For detection of activated proteins, RIPA lysates from the same collections were separated by SDS–PAGE, transferred to a PVDF membrane (0.2 μm) and probed with appropriate antiserum as previously described. Finally, probing with primary antibody against immunoprecipitation antibody and subsequent species specific secondary antibody were used to verify equal protein loading.

BCL-2 protein cellular delivery

Recombinant biologically functional BCL-2 protein (R&D Systems Inc., Minneapolis, MN, USA) was delivered into COLO 205 cells with SAINT-PhD [1-methyl-4-(cis-9-dioleyl)methylpyridinium-chloride (SAINT-18) 1,2-Dioleyl-sn-glycero-3-phosphoethanolamine (DOPE)] reagent according to the producer's indications (Synvolux Therapeutics, Groningen, The Netherlands). For WB analysis cells were cultured on 60 mm Petri dish. When cells became confluent the profection procedure was performed. A 20 μg of BCL-2 protein was diluted with the HEPES buffered salt (HBS buffer, pH 7.4) to achieve a volume of 300 μl. Then, 200 μl of SAINT-PhD into protein/HBS solution was added. The mixture was filled up to 2.5 ml with 10% FBS/DMEM medium. Just prior to profection the medium was aspirated and cells were washed once with HBS. Then SAINT-PhD/protein complexes were overlaid onto the washed cells and incubated at 37°C for 4 h. After incubation the transfection mixture was filled up to 4 ml with extra medium. When performing profection in culture plates of various sizes the quantity of HBS and SAINT-PhD reagents were scaled in proportion to the surface area of the plate. In case of WB analysis the level of BCL-2 protein was examined 24 h after transfection. For MTT assay, when transfection procedure was completed, cells were treated with tested compounds and cell viability was evaluated at 6, 12 or 24 h of experiment.

siRNA transfection protocol

siRNA CTRL (siCTRL) or siRNA BCL-2 (siBCL-2) or siRNA FLIP (siFLIP) (Santa Cruz Biotechnology, Santa Cruz, CA, USA) were delivered into the cells with SAINT-RED [1-methyl-4-(cis-9-dioleyl)methyl-pyridinium-chlorid (SAINT-18) and dioleoyl-phosphatidylethanolamine (DOPE)] reagent according to the producer's protocol (Synvolux Therapeutics, Groningen, The Netherlands). Transfection was performed in 96-well plate. For one well, 3 pmol of appropriate siRNA was diluted with 6 μl of HEPES buffered salt (HBS buffer, pH 7.4). At the same time, 1.25 μl of SAINT-RED was diluted with 5 μl of HBS buffer. Both mixtures were mixed together after 5 min incubation. siRNA/SAINT-RED complexes volume was filled up to 65 μl of 10% FCS/DMEM and the solution was overlaid onto the washed cells and incubated at 37°C for additional 3 h. After incubation the transfection mixture was filled up with 125 μl with extra medium and cells were incubated for 72 h. For MTT assay, when transfection procedure was completed, cells were treated with tested compounds and cell viability was evaluated at 6, 12 or 24 h of experiment.

Statistical analysis

Each treatment was carried out at least in triplicate and each experiment was repeated at least twice with similar results. The results were statistically evaluated with one-way ANOVA and Tukey's multiple range test when compared to control treatments. These analyses were performed using GraphPad Prism™ version 4.03 software (GraphPad Software Inc., San Diego, CA, USA). In order to show the quantitative differences, the percentage of initial control value was set arbitrarily as 100% (experimental value/initial control value × 100) at each time point used. Statistical differences were interpreted as significant at $P < 0.05$ and highly significant at $P < 0.01$.

Results

Sodium butyrate potentiates TNF-α-mediated apoptosis

Examination of human colon adenocarcinoma COLO 205 cells revealed that upon treatment with NaBt [2 mM] the cells became highly sensitive to the apoptotic effect of TNF-α (Fig. 1). Irrespective to the presence of functional TNF-R1 receptors on plasma membrane of COLO 205 cells [21] it was previously reported that the cells are resistant to apoptotic stimuli induced by TNF-α [13]. Therefore, it is obvious why the incubation of COLO 205 cells with a physiological concentration of TNF-α [10 ng/ml] had no detectable effect on cell morphology (Fig. 1a), apoptosis induction (Fig. 1b) or procaspase-3 level (Fig. 1c) compared to that of control cells. In contrast, after incubation with both TNF-α [10 ng/ml] and NaBt [2 mM] a significant number of cells became round-shaped, with apparent membrane blebbing and condensed nuclei (Fig. 1d). Overall, these changes are typical for apoptosis detected at least in the 6th hour of experiment (Fig. 1b). The apoptotic index (AI) ranged from 1.08 ± 0.18 for control to 20.05 ± 0.12, 36.11 ± 3.12 and 67.09 ± 6.15 for concomitant TNF-α and NaBt treatment at 6, 12 and

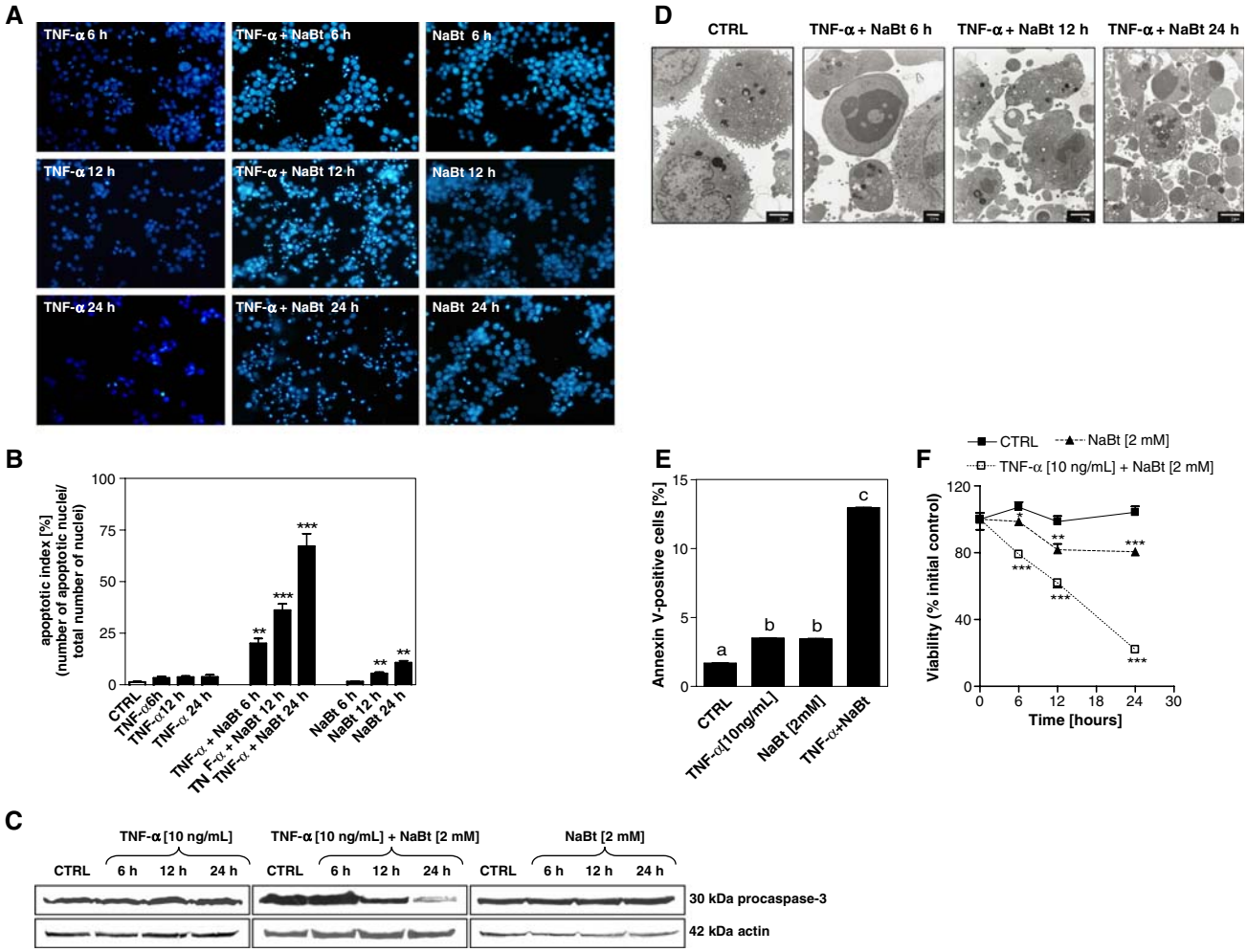

Fig. 1 Sodium butyrate sensitizes COLO 205 cells to TNF-α-induced apoptosis. **a** Series of images of COLO 205 cells obtained from fluorescent microscope under UV light. Nuclear chromatin is shown after serial staining with bisbenzimide/propidium iodide (see "Materials and methods" section). No chromatin condensation was detected after TNF-α treatment [10 ng/ml] irrespective to incubation time (6, 12 and 24 h). In contrast, TNF-α [10 ng/ml] and NaBt [2 mM] co-treatment induced both chromatin condensation and fragmentation of nuclei. While NaBt [2 mM] alone has minimal effect on apoptosis of COLO 205 cells, NaBt treatment [2 mM] induced significant increase in both chromatin condensation and nuclei fragmentation (at least in the 12th hour of experiment). Images were acquired under ×20 lens and ×5 digital zoom. **b** *Bar charts* representing apoptotic indices (AI) calculated for TNF-α amounted to 2.95 ± 0.41, 3.27 ± 0.74 and 3.71 ± 0.59 ($P > 0.05$) in the 6th, 12th and 24th hour of treatment, respectively; for TNF-α + NaBt [2 mM] amounted to 20.05 ± 2.38, 36.112 ± 3.11 and 67.09 ± 6.15 in the 6th, 12th and 24th hour of treatment, respectively; and for NaBt [2 mM] amounted to 1.50 ± 0.24, 5.423 ± 0.69 and 10.68 ± 0.96 at 6th, 12th and 24th hour of treatment, respectively. Significant differences between the treatment means and control value are indicated by $*P < 0.05$, $**P < 0.01$ and $***P < 0.001$. **c** Western-blot analyses of whole-cell lysates obtained from COLO 205 cells. Immunoblots show the expression of procaspase-3 protein after individual TNF-α [10 ng/ml] and NaBt [2 mM] as well as combined TNF-α + NaBt [10 ng/ml + 2 mM, respectively] treatment at 6, 12 and 24 h. Each experiment was repeated at least twice with similar results. **d** Electron microscopy evaluation of NaBt-mediated [2 mM] sensitization to TNF-α-induced [10 ng/ml] apoptosis. From left to right: control cell ultrastructurally unchanged containing nucleus and cytoplasm rich in mitochondria and other unchanged organelles, bar—2 μm; the early apoptotic cell; cells exhibiting nuclear condensation and fragmentation, cell shrinkage and ruffled nuclear and cell membranes; the cytoplasmic condensation with ribosome loss from rough endoplasmic reticulum is present in the 6th hour of combined treatment with TNF-α and NaBt [2 mM]. Note fragments of ultrastructurally unchanged COLO 205 cell in the vicinity to apoptotic cell, bar—1 μm; typical apoptotic cell; note pyknosis of nucleus with chromatin and cytoplasmic condensation, cell fragmentation to apoptotic bodies in the 12th hour of combined treatment with TNF-α and NaBt [2 mM], bar—2 μm; late apoptotic cells; very small cells containing condensed, or "non-transparent" chromatin, which is segregated into crescents and caps. Cells are disintegrated into apoptotic bodies in the 24th hour of combined treatment with TNF-α and NaBt [2 mM], bar—2 μm. **e** Flow cytometry analysis using Annexin V/PI staining of apoptotic/necrotic cells after 4 h exposure to TNF-α [10 ng/ml] or NaBt [2 mM] or TNF-α [10 ng/ml] + NaBt [2 mM]. Each experiment was repeated at least twice with similar results. **f** MTT assay showing the effects of NaBt [2 mM (▲)] or TNF-α [10 ng/ml] and NaBt [2 mM] (□) co-treatment (6, 12, 24 h) on the viability of COLO 205 cells. Significant differences between the treatment means and control values at respective times are indicated by $*P < 0.05$, $**P < 0.01$ and $***P < 0.001$. Values represent means from two identical experiments carried out in quadruplicates ± SEM

24 h, respectively (Fig. 1b). Additionally, apoptosis induction was confirmed by flow cytometry where the percentage of annexin V-positive cells after 4 h of experiment was measured (Fig. 1e). Also MTT assay confirmed that cell death progressed as the reduced viability of COLO 205 cells was observed (Fig. 1f). Accordingly, the hallmarks of apoptosis were corroborated with SDS–PAGE and immunoblotting which showed time-dependent reduction of procaspase-3 level (Fig. 1c). Cytochemistry analysis (PI/HO33342 staining), apoptotic index and flow cytometry study, they all indicated, that NaBt [2 mM] was apparently not apoptotic unless TNF-α was added (Fig. 1). At higher concentration of NaBt [5 or 10 mM] an additional reduction of cell viability was observed and apoptosis was executed (Fig. 2). Anyway, in order to investigate the potency of NaBt to overcome resistance of COLO 205 cells to TNF-α, 2 mM was used as the highest non-toxic NaBt concentration in a combination with TNF-α. Presented data clearly show that combined treatment with NaBt [2 mM] and TNF-α [10 ng/ml] resulted in a rapid and extensive death of COLO 205 cells.

Sodium butyrate facilitates extrinsic apoptosis by reduction of the cFLIP protein level and up-regulation of TNF-R1 protein in COLO 205 cell line

Based on our previous observations that COLO 205 cells could be sensititized to TNF-α-mediated apoptosis by the metabolic inhibitors, such as cycloheximide (CHX) [13] or bisindolylmaleimide IX (Bis-IX) [22] we performed both WB and immunoprecipitation studies to examine the influence of TNF-α [10 ng/ml] or NaBt [2 mM] or TNF-α

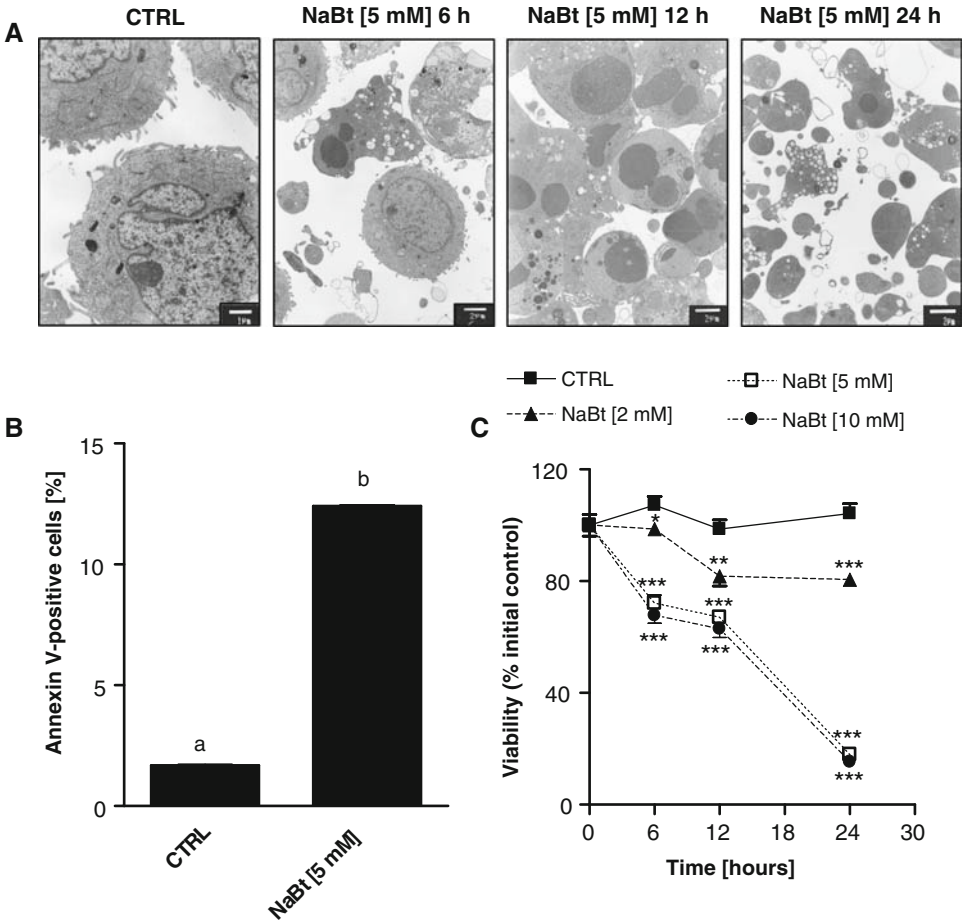

Fig. 2 Higher concentration of NaBt [5 mM] induces apoptosis of COLO 205 cells, irrespective to TNF-α. **a** Electron microscopy evaluation of NaBt-induced [5 mM] apoptosis. From left to right: control ultrastructurally unchanged cells, bar—1 μm; COLO 205 cells after following hours (6, 12 and 24 h) of NaBt [5 mM] treatment, showing hallmarks of typical apoptosis, such as pyknosis of nucleus, nuclear condensation and fragmentation, cell shrinkage and fragmentation to apoptotic bodies, bar 2 μm. **b** Flow cytometry analysis using Annexin V/PI staining of apoptotic/necrotic cells after 4 h of NaBt [5 mM] treatment. Each experiment was repeated at least twice with similar results. **c** MTT assay showing dose-response effect to NaBt [2 mM (▲), or 5 mM (□), or 10 mM (●)] in COLO 205 cells. Significant differences between the treatment means and control values at respective times are indicated by $*P < 0.05$, $**P < 0.01$ and $***P < 0.001$. Values represent means from two identical experiments carried out in quadruplicates ± SEM

[10 ng/ml] + NaBt [2 mM] on the level of cFLIP protein. Additionally, we decided to determine the level of other TNF-R1-DISC (death initiating signaling complex) components, such as TNF-R1, TRADD and FADD, and proteins mediating TNF-α-dependent NF-κB activation (TRAF2, cIAP-1, RIP). As shown on Fig. 3a, the combined TNF-α and NaBt [2 mM] treatment resulted in a time-dependent decline in cFLIP protein level. Furthermore, the immunoprecipitation analysis confirmed that cFLIP level was diminished in DISC complex (Fig. 3b). Similarly, cFLIP protein expression was dramatically down-regulated when cells were treated individually with NaBt [2 mM] (Fig. 3a, b). Crucial role of cFLIP in the resistance to TNF-α was confirmed by siRNA transfection procedure. According to MTT assay, *FLIP* knock-down was sufficient to sensitize COLO 205 cells to TNF-α-induced cell death (Fig. 3c). Furthermore, NaBt [2 mM] and concomitant TNF-α + NaBt [2 mM], but not TNF-α [10 ng/ml] treatments affected the level of TNF-R1. The expression of TNF-R1 was strongly up-regulated, especially after 24 h of incubation (Fig. 3a). On the other hand, the levels of other DISC components: FADD, TRADD remained intact, regardless of tested compound(s). Importantly, neither treatment modulated the expression of proteins involved in

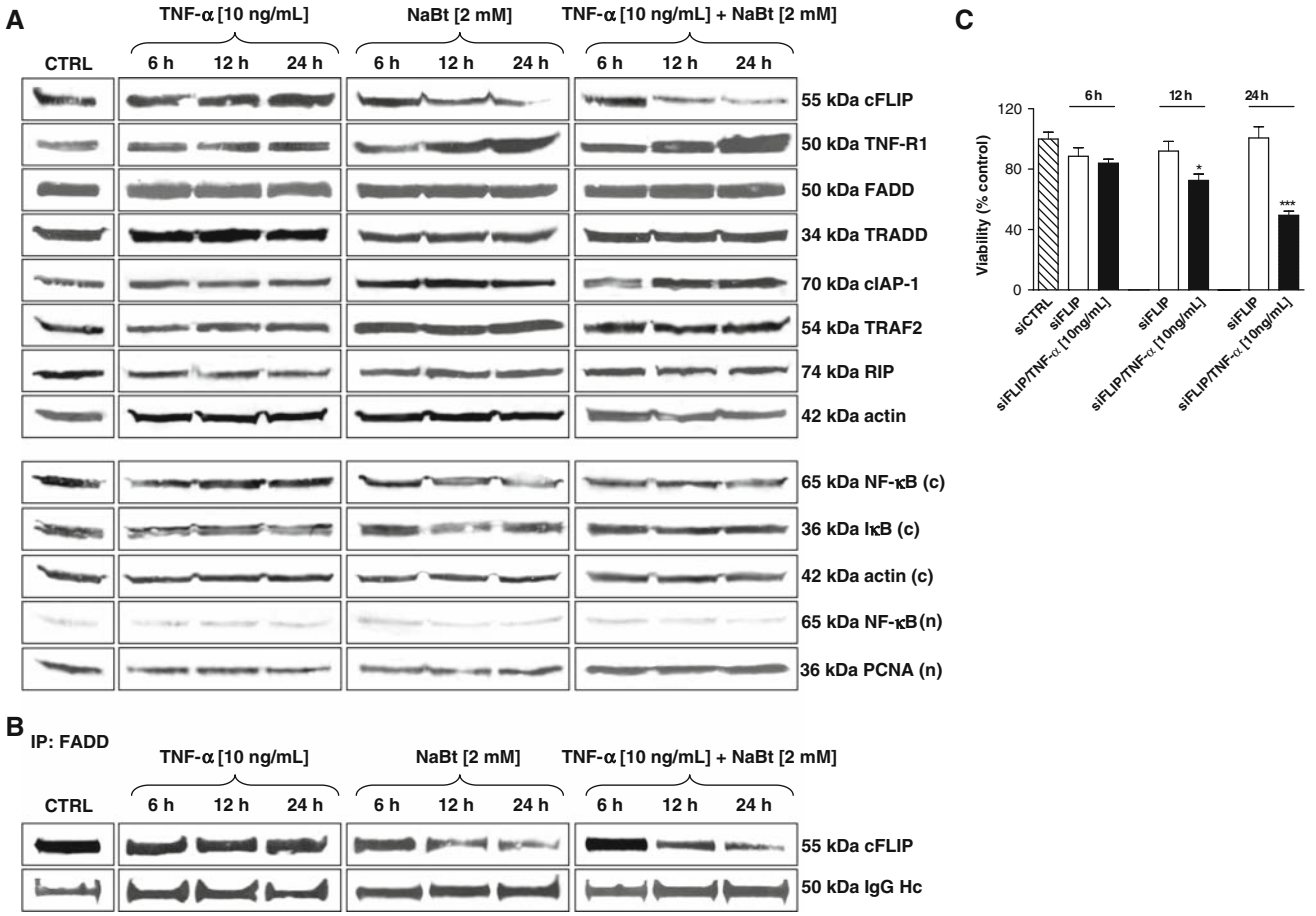

Fig. 3 NaBt [2 mM] treatment affects the expression of TNF-R1-DISC components, but not TNF-α-dependent NF-κB pathway. **a** Western-blot analyses of whole-cell or cytoplasmic and nuclear lysates obtained from COLO 205 cells are shown. Immunoblots represent the expression of cFLIP, TRADD, FADD,TNF-R1, cIAP-1, TRAF2 and RIP proteins after TNF-α [10 ng/ml] or NaBt [2 mM] or TNF-α [10 ng/ml] + NaBt [2 mM] at 6, 12 and 24 h of treatments. Membranes were also probed with anti-actin antibody to normalize protein levels. Below, immunoblots represent the expression of NF-κB and IκBα in cytoplasmic (c) and NF-κB in nuclear (n) fractions. The cytoplasmic protein expression was compared to actin level, whereas the level of nuclear proteins was normalized with respect to PCNA expression. Each experiment was repeated at least twice with similar results. **b** The analysis of protein–protein interactions is shown by immunoprecipitation. The whole-cell lysates obtained from COLO 205 cells treated with TNF-α [10 ng/ml] or NaBt [2 mM] or TNF-α [10 ng/ml] + NaBt [2 mM] at 6, 12 and 24 h versus untreated cells (CTRL) were immunoprecipitated with anti-FADD antibody absorbed on A/G agarose beads. cFLIP protein was detected by immunoblotting following electrophoresis of the cell lysates. Each experiment was repeated at least twice with similar results. **c** MTT assay showing the effect of TNF-α [10 ng/ml] treatment (6, 12, 24 h) on viability of COLO 205 cells after siRNA *FLIP* transfection. Significant differences between the treatment means and control values at respective times are indicated by $*P < 0.05$, $**P < 0.01$ and $***P < 0.001$. Values represent means from two identical experiments carried out in quadruplicates ± SEM

NF-κB signaling pathway, such as TRAF2, RIP and cIAP-1. At the same time, no visible changes in NF-κB and IκB protein levels were observed.

Higher expression of the specific transmembrane TNF-α receptor (TNF-R1), as well as lower immunoreactivity of antiapoptotic cFLIP protein lead TNF-α to activate extrinsic apoptotic pathway. As a consequence the caspase-8 and 3 were activated (Fig. 4a). In the presence of NaBt [2 mM], the TNF-α-dependent death signal was also transmitted to mitochondria by caspase-8-dependent BID cleavage (tBID). Moreover, cytochrome *c* was released and caspase-9 became activated (Fig. 4a). No such changes in protein expression were detectable after individual TNF-α [10 ng/ml] or NaBt [2 mM] administration, irrespective to the time of incubation (Fig. 4a). Combined TNF-α and NaBt cytotoxic effect was abolished when z-IETD-fmk [20 μM] (caspase 8 irreversible inhibitor) was administrated, and was further confirmed by WB, MTT and flow cytometry analysis (Fig. 4). Our findings clearly demonstrate that in the presence of NaBt [2 mM] TNF-α is able to initiate apoptotic death of COLO 205 cells.

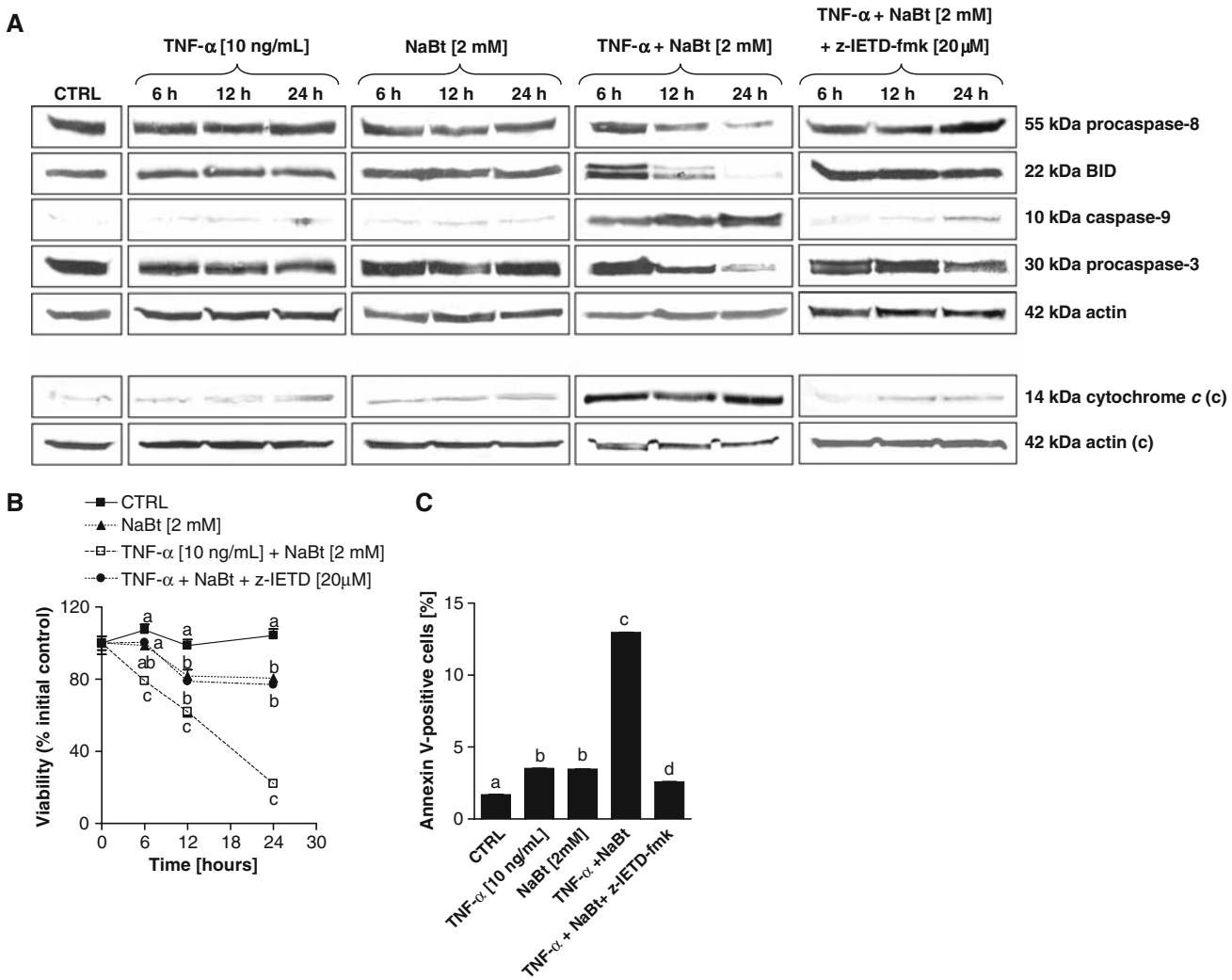

Fig. 4 TNF-α [10 ng/ml] + NaBt [2 mM]-mediated activation of extrinsic apoptotic pathway is potentiated by mitochondria in COLO 205 cells. **a** Western-blot analyses of whole-cell or cytosolic lysates obtained from COLO 205 cells. Immunoblots showing the expression of procaspase-8, caspase-9, BID, procaspase-3 and cytochrome *c* proteins after TNF-α [10 ng/ml] or NaBt [2 mM] or combined TNF-α [10 ng/ml] + NaBt [2 mM] treatments (6, 12 and 24 h) without or in the presence of dominant negative caspase-8 inhibitor (z-IETD-fmk) [20 μM]. Membranes were also probed with anti-actin antibody to normalize protein levels. Each experiment was repeated at least twice with similar results. **b** MTT assay showing viability of COLO 205 cells after: NaBt [2 mM] (▲), or TNF-α [10 ng/ml] + NaBt [2 mM] (□), or TNF-α [10 ng/ml] + NaBt [2 mM] + z-IETD-fmk [20 μM] (■) treatment. Means ± SEM bearing different small letters within particular treatment time differ at least significantly $P < 0.05$. Values represent means from two identical experiments carried out in quadruplicates. **c** Flow cytometry analysis using Annexin V/PI staining of apoptotic/necrotic cells after 4 h of TNF-α [10 ng/ml] + NaBt [2 mM] or TNF-α [10 ng/ml] + NaBt [2 mM] + z-IETD-fmk [20 μM] treatment. Each experiment was repeated at least twice with similar results

Sodium butyrate initiates intrinsic apoptotic pathway by modulation of apoptosis-related protein expression

As shown on Fig. 2, irrespective to TNF-α, higher concentration of NaBt alone significantly reduced cell viability with consequent apoptosis induction, as confirmed by annexin V/PI staining and considerable changes in cell ultrastructure. We found that observed cytotoxic effect of NaBt resulted from activation of caspases (Fig. 5a–c). Thus, as we expected the presence of pan-caspase inhibitor—z-VAD-fmk [20 μM] protected COLO 205 cells from NaBt [5 mM]-induced cell death. The preventive effect of z-VAD-fmk was demonstrated by indices of WB, MTT and flow cytometry analysis (Fig. 5a–c). Consistently, NaBt treatment [5 mM] resulted in up-regulation of caspase-9 which was accompanied by a fall in procaspase-3 level as shown by WB analysis. Simultaneously, no changes in procaspase-8 level were observed, however, at the same time, cytochrome *c* was detected in the cytoplasm. In the presence of z-VAD-fmk [10 μM], NaBt-induced [5 mM] activation of caspases and release of cytochrome *c* to cytoplasm were not detected (Fig. 5a). The involvement of mitochondria in NaBt-dependent apoptosis was verified by BCL-2 protein intracellular delivery. As shown on Fig. 5d,

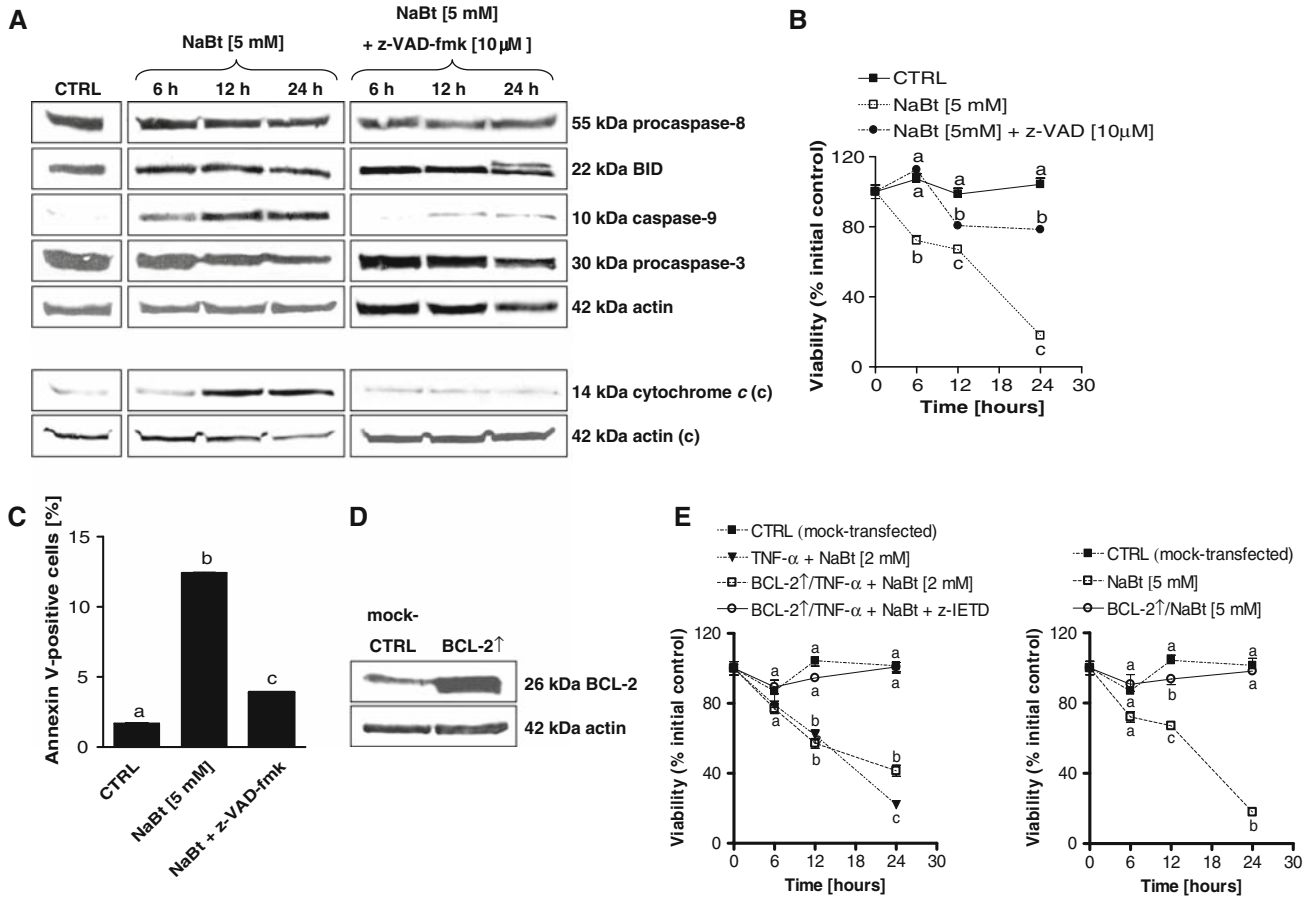

Fig. 5 NaBt [5 mM] activates intrinsic apoptotic pathway, which is abolished by BCL-2 overexpression. **a** Western-blot analyses of whole-cell or cytosolic lysates were obtained from COLO 205 cells. Immunoblots showing the expression of procaspase-8, caspase-9, BID, procaspase-3, cytochrome *c* proteins after NaBt [5 mM], or NaBt [5 mM] + z-VAD-fmk [10 μM] co-treatment (6, 12 and 24 h). Membranes were also probed with anti-actin antibody to normalize protein levels. Each experiment was repeated at least twice with similar results. **b** MTT assay showing viability of COLO 205 cells after NaBt [5 mM] (□), or NaBt [5 mM] and z-VAD-fmk [10 μM] treatment. Means ± SEM bearing different small letters within particular treatment time differ at least significantly $P < 0.05$. Values represent means from two identical experiments carried out in quadruplicates. **c** Flow cytometry analysis using Annexin V/PI staining of apoptotic/necrotic cells after 4 h of NaBt [5 mM] or NaBt [5 mM] + z-VAD-fmk [10 μM] treatment. Each experiment was repeated at least twice with similar results. **d** Immunoblots showing the expression of BCL-2 protein at 24th hour after mock- or BCL-2-transfection. Membranes were also probed with anti-actin antibody to normalize protein level. Data are representative values. **e** *Left*: MTT assay showing viability of COLO 205 cells after TNF-α [10 ng/ml] and NaBt [2 mM] (▼) co-treatment in comparison with viability of BCL-2-transfected cells treated with TNF-α [10 ng/ml] and NaBt [2 mM] (□), or TNF-α [10 ng/ml] and NaBt [2 mM] and z-IETD-fmk [20 μM] (○); *Right*: MTT assay showing viability after NaBt treatment [5 mM] in non- (□) or BCL-2-transfected (○) COLO 205 cells. Means ± SEM bearing different small letters within particular treatment time differ at least significantly $P < 0.05$. Values represent means from two identical experiments carried out in quadruplicates

profection with BCL-2 resulted in the intracellularly elevated level of biologically functional BCL-2 protein. Nevertheless, increased BCL-2 protein level could not prevent TNF-α and NaBt-induced apoptosis, at least at 6 and 12 h of experiment (Fig. 5e). Finally, the concomitant BCL-2 delivery and z-IETD-fmk [20 μM] administration fully protected COLO 205 cells from TNF-α and NaBt-induced apoptosis (Fig. 5e). It suggests that extrinsic apoptotic pathway was amplified by mitochondria, but mitochondria were not essential for TNF-α and NaBt-induced COLO 205 cell deletion. In contrast, BCL-2 delivery efficiently blocked NaBt-dependent [5 mM] cytotoxic effect (Fig. 5e). The viability of BCL-2-transfected COLO 205 cells upon NaBt [5 mM] stimulation was almost similar to that of control cells. We concluded that the main target of NaBt [5 mM] alone was situated in the intrinsic apoptotic pathway. Interestingly, BCL-2 protein overexpression was sufficient to protect COLO 205 cells from NaBt [5 mM]-induced cell death, whereas *BCL-2* down-regulation by the use of siRNA did not permit NaBt at lower concentration [2 mM] to induce apoptosis (Fig. 6a). Consequently, we examined whether NaBt-induced apoptosis [5 mM] was associated with changes in the levels of other apoptosis-related proteins. BCL-2 and BAX protein levels were not altered in the presence of NaBt [5 mM], whereas this treatment resulted in down-regulation of BCL-x_L and concomitant up-regulation of BAK proteins (Fig. 6b) in COLO 205 cells. Protein levels of two major IAP proteins, survivin and XIAP were also significantly reduced upon NaBt-induced [5 mM] apoptosis (Fig. 6b). Since many antiapoptotic proteins, including XIAP and BCL-x_L are substrates for caspases [23, 24], we examined if the levels of these proteins are somehow correlated with caspases activation. Hence, we evaluated the expression of apoptosis-related proteins in the presence of NaBt [5 mM] and pan-caspase inhibitor z-VAD-fmk [10 μM]. As shown on Fig. 6b, in spite of caspases inhibition, the antiapoptotic proteins levels, such as BCL-x_L, XIAP and survivin were still diminished upon treatment. These results suggest, that another non-caspase controlled mechanism may exist with regard to NaBt-dependent regulation of these proteins in COLO 205 cells.

Discussion

One promising tool for treating tumor cells which are resistant to apoptosis is to make use of the cytotoxic drugs which could sensitize cancer cells to physiological death stimuli [25, 26]. From this point of view, sodium butyrate (NaBt) is believed to modulate the resistance of human colon adenocarcinoma COLO 205 cells to TNF-α-induced apoptosis [21, 27]. Cytotoxic drugs often induce cell death via the up-regulation of death receptors [28]. In this case, we found that the expression of TNF-R1 was up-regulated, especially after 24 h of co-treatment with TNF-α and NaBt [2 mM] (Fig. 3a). Our results are in agreement with observations reported by Chopin et al. [29] and Nakata

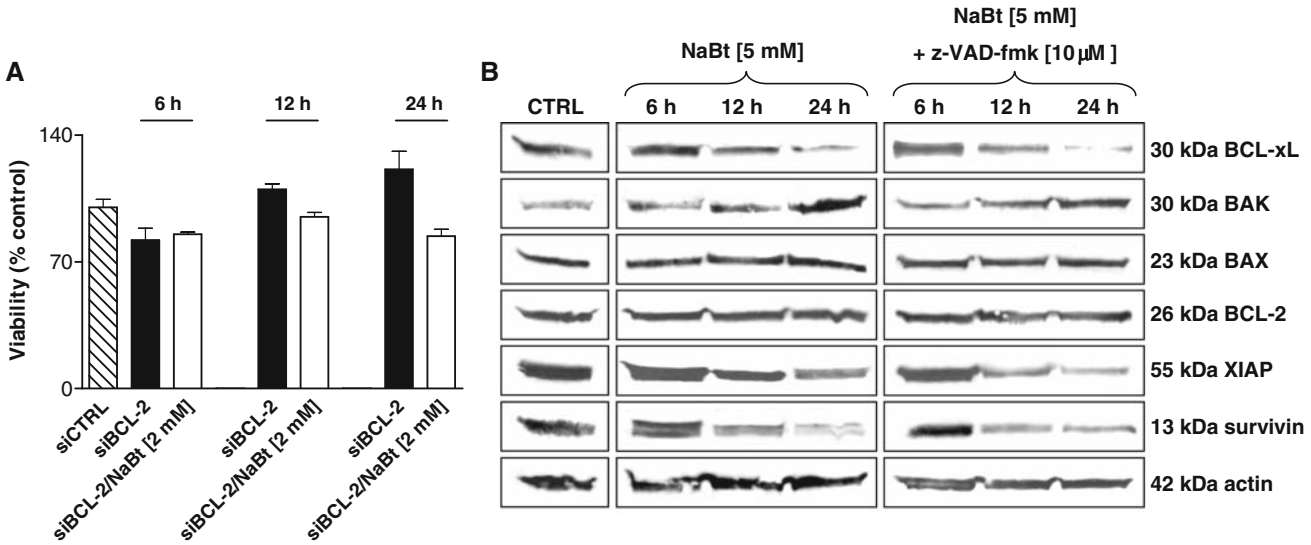

Fig. 6 NaBt [5 mM] facilitates intrinsic apoptosis by modulated expression of apoptosis-related proteins. **a** MTT assay showing the effect of NaBt [2 mM] treatment (6, 12, 24 h) on viability of COLO 205 cells after siRNA BCL-2 transfection. Significant differences between the treatment means and control values at respective times are indicated by $*P < 0.05$, $**P < 0.01$ and $***P < 0.001$. Values represent means from two identical experiments carried out in quadruplicates ± SEM. **b** Western-blot analyses of whole-cell or cytosolic lysates were obtained from COLO 205 cells. Immunoblots showing the expression of BCL-x_L, BAK, BAX, BCL-2, XIAP and survivin proteins after NaBt [5 mM], or NaBt [5 mM] + z-VAD-fmk [10 μM] co-treatment (6, 12 and 24 h). Membranes were also probed with anti-actin antibody to normalize protein levels. Each experiment was repeated at least twice with similar results

et al. [30]. Chopin et al. [29] demonstrated that NaBt significantly potentiated the expression of TNF-R1, TNF-R2, TRAIL-R1, TRAIL-R2 and Fas death receptors, at least in the 24th hour of treatment of breast cancer cells. The NaBt-mediated facilitation of TNF-α-induced death signal was further supported by the repression of factor(s) which inhibited death signal cascade. Indeed, some of our previous results demonstrated that COLO 205 cells are refractory to TNF-α-induced apoptosis due to the inhibited caspase-8 activation by the cFLIP protein [13, 22, 27]. In this study we verified our hypothesis if NaBt could facilitate TNF-α-induced cell death. WB and immunoprecipitation studies were performed to evaluate the levels of TNF-R1 signalosome components, such as cFLIP, TRADD, FADD, RIP, TRAF2 and cIAP-1 after TNF-α [10 ng/ml], NaBt [2 mM] and combined TNF-α + NaBt administration. As shown on Fig. 3, the presence of NaBt [2 mM], but not TNF-α [10 ng/ml], resulted in a time-dependent down-regulation of cFLIP protein, whereas the levels of other signalosome components were not affected (Fig. 3a). Moreover, the knock-down of *FLIP* restored the susceptibility of COLO 205 cells to the apoptotic signal from TNF-R1. The modulation of cFLIP protein by NaBt was previously reported by Pajak and Orzechowski [27], Natoni et al. [16] and Hernandez et al. [14]. Consistent with our observations Natoni et al. [16] and Hernandez et al. [14] reported that 24 h of NaBt treatment resulted in dramatic reduction of cFLIP protein (Fig. 3). On the other hand, Kim et al. [31] did not observe any changes in the expression of cFLIP protein upon NaBt treatment of glioma cells. We assumed that cytotoxic effects of NaBt are cell type specific. However, we concluded that NaBt-mediated overexpression of transmembrane TNF-R1 and concomitant drop of cFLIP protein, may contribute to the restored sensitivity of COLO 205 cells to TNF-α. Consequently, the TNF-α [10 ng/ml] and NaBt [2 mM] administration resulted in rapid cell apoptosis (Fig. 1).

Regardless of its proapoptotic effect, TNF-α is also known as a potent activator of NF-κB transcription factor. However, we have previously shown that in COLO 205 cells TNF-α-dependent NF-κB activation occurs only in the additional presence of interferon α (IFN-α) [32]. Thus, it was not surprising that NaBt did not modulate the expression of TNF-R1 signalosome components such as TRAF2, cIAP-1 and RIP and had no influence on the cytoplasmic or nuclear level of NF-κB protein (Fig. 3). Consequently, proapoptotic action of NaBt and TNF-α-induced death signal in COLO 205 cells were chosen for further examination.

The present study illustrates also the effect of NaBt in conjunction with the mitochondria-dependent apoptotic pathway. As shown on Fig. 4a, combined NaBt [2 mM] and TNF-α treatment led to both the procaspase-8 and BID cleavages. At the same time, the cytochrome *c* was released from mitochondria and caspase-9 was activated. No such effects were observed when cells were treated with TNF-α [10 g/ml] or NaBt [2 mM] alone. Most likely, BID and procaspase-9 cleavages resulted from the extrinsic apoptotic cascade activation in COLO 205 cells. BID cleavage is processed by caspase-8 in DISC complex (type II cell death) [33, 34]. The truncated Bid (tBID) is able to translocate to the mitochondrial membrane where it is complexed with BAX and a voltage-dependent anion channel (VDAC). Such complexes allow the release of mitochondrial components of apoptosome (dATP, cytochrome *c*). Next, apoptosome triggers procaspase-9 conversion into active caspase-9. To verify whether the observed changes in BID, caspase-9 and cytochrome *c* levels are associated with extrinsic apoptosis, the caspase-8 inhibitor (z-IETD-fmk) has been used. Z-IETD-fmk prevented BID and procaspase-8 cleavage (Fig. 4a). Furthermore, caspase-9 was not activated and cytochrome *c* was not released (Fig. 4a). Additionally, cell viability was significantly elevated when compared to TNF-α and NaBt [2 mM] co-treatment and was not significantly different from NaBt [2 mM] alone (Fig. 4b). Moreover, significantly lower percentage of annexin V-positive cells was detected by flow cytometry (Fig. 4c). To verify which molecular mechanism: type I or type II cell death is in favor by the combination of TNF-α and NaBt [2 mM], COLO 205 cells were transfected with functional recombinant BCL-2 protein, which counteracts the mitochondria-mediated apoptosis. According to MTT assay, the overexpression of BCL-2 had no effect on TNF-α and NaBt [2 mM]-induced apoptosis during 12 h of experiment. The protective effect of BCL-2 was detectable only at 24th hour of treatment, even then, however, the viability of COLO 205 cells was reduced by almost 50% (Fig. 5e). It indicates that direct activation of caspase-3 by caspase-8 determines the potent cytotoxic effect of combined treatment of TNF-α and NaBt [2 mM].

As shown on Fig. 2, higher concentrations of NaBt [5 and 10 mM] led to significant decrease in cell viability. In these circumstances, the concomitant use of pan-caspase inhibitor z-VAD-fmk significantly restored cell viability (Fig. 5b). In consequence, it appeared that cell mortality was caused by caspase-dependent cell death. Interestingly, the curves illustrating viability of NaBt [5 mM] and z-VAD-fmk [10 μM]-treated cells were similar to that of TNF-α [10 ng/ml] and NaBt [2 mM] and z-IETD-fmk [20 μM]-treated cells. In both cases cells were effectively protected from caspase activation, however at 12th and 24th hours cell survival was diminished by about 20% (Figs. 4b, 5b) in comparison to control cells. It suggests that the observed cytotoxic effect of NaBt does not depend on caspase activation. Examination by TEM did not

provide any hallmarks of autophagy or necrosis in cell ultrastructure. Furthermore, flow cytometry analysis of annexin V/PI-stained COLO 205 cells after 4 h of experiment, detected merely 1% of necrotic cells, regardless of treatment (TNF-α [10 ng/ml] or NaBt [2, 5 mM] or TNF-α + NaBt [2 mM]) (data not shown). Thus, it is possible that NaBt initiates additional caspase-independent apoptotic pathway. Caspase-independent apoptosis is known to be mediated by three major pathways: p53-, or calpains-, or AIF-dependent pathway [35–38]. Interestingly, Wu et al. [38] demonstrated that histone deacetylase inhibitor—trichostatin A (TSA) was able to activate caspase-independent programed cell death (PCD) in gastric cancer cells via AIF and EndoG translocation from mitochondria to nucleus. It is probable that sodium butyrate, as a HDAC inhibitor, triggers the same pathway in colon cancer cells. Therefore, the identification of additional molecular mechanisms of NaBt cytotoxic action would by highly desired.

With regard to NaBt-induced apoptosis [5 mM], we performed WB analysis. As showed on Fig. 5a, NaBt [5 mM] treatment caused time-dependent increase in immunoreactivity of cleaved form of caspase-9 and drop in procaspase-3 level, whereas it did not affect procaspase-8 and BID protein. At the same time, the presence of cytochrome *c* in the cytoplasm was detected. Based on presented results we conclude that NaBt [5 mM] initiated intrinsic apoptotic pathway. No such changes in protein expression were detected when NaBt [5 mM] was used with z-VAD-fmk [10 μM] (Fig. 5a). Finally, the contribution of mitochondria to apoptosis was positively verified by BCL-2 transfection. Overexpression of antiapoptotic BCL-2 protein mimicked the antiapoptotic effect of z-VAD-fmk (Fig. 5e). The role of intrinsic apoptosis in NaBt cytotoxic action was also confirmed by other reports, such as by Ruemmele et al. [39] and by Natoni et al. [16]. Ruemmele et al. [39] claimed that NaBt administration decreased BCL-x_L and up-regulated BAK expression in a potent and a dose-dependent manner. Increased levels of BAK are known to allow exit of cytochrome *c* from the mitochondria to the cytoplasmic compartment [40]. Based on previous results of Schimizu et al. [40], Ruemmele et al. [39] hypothesized that cytochrome *c* is released from mitochondria by VDAC channel, activity of which is dependent on the conformational changes induced by functional BH3 region of BAK or BAX proteins. Interestingly, BCL-x_L was a competitive inhibitor of BAK effect on VDAC. In the presence of BCL-x_L, cytochrome *c* release was dramatically inhibited. Based on described results, Ruemmele et al. [39] proposed that this pathway could explain the NaBt-mediated intrinsic apoptosis in glioma cells. On the other hand, Natoni et al. [16] suggested, that the release of proapoptotic proteins from mitochondrial intermembrane space to the cytosol is determined by mitochondrial membrane depolarization. Florescent probe JC-1 revealed that reduced mitochondrial potential was detectable after 48 h of NaBt treatment and reached high levels at 72 h [16]. At the same time, WB and RT-PCR analysis showed the time-dependent and strong reduction of BCL-x_L expression upon NaBt [5 mM] treatment. It corroborated results of Ruemmele et al. [39]. It is obvious that in the NaBt-treated cells, intrinsic apoptotic pathway is initiated by down-regulation of antiapoptotic (BCL-x_L) and up-regulation of proapoptotic (BAK) proteins. Elevated level of BAK allows extensive BAK-BAX complexes formation and thus stimulates the release of apoptotic factors from mitochondria [41]. Accordingly, NaBt-mediated death signal from mitochondria could be retarded when the antiapoptotic BCL-2 proteins repress BAK or BAX. In accordance to our studies, WB analysis confirmed that analogous mechanism could explain the cytotoxic effect of NaBt [5 mM]. In Fig. 6, the down-regulation of BCL-x_L and concomitant induction of BAK expression occurred during following hours of NaBt [5 mM] treatment. Interestingly, *BCL-2* down-regulation by siRNA was not able to sensitize COLO 205 cells to lower concentration of NaBt [2 mM] (Fig. 6a). Thus, we concluded that the balance between BCL-2 and BAK proteins is crucial for intrinsic apoptosis execution. This hypothesis elucidate the observation how BCL-2 cellular delivery fully protected COLO 205 cells from NaBt-induced [5 mM] caspase-dependent cell death.

Described observations suggested also that NaBt [5 mM] proapoptotic effect is not mediated by modulation of p53 activity. It is known, that BCL-2 and BAX proteins expression is regulated by p53 [42]. One of the identified mechanisms controlling p53 transcriptional activity is its posttranslational acetylation at C-terminal domain [43, 44]. According to Juan et al. [45], p53 acetylation prolongs, whereas histone deacetylases inhibits p53-dependent gene activation. Hence, the inhibition of histone deacetylases by NaBt should result in constitutive expression of BCL-2 and BAX proteins. Consequently, after 24 h of NaBt [5 mM] action it would be sufficient to detect the cellular accumulation of BCL-2 and BAX proteins in COLO 205 cells. However, according to WB analysis (Fig. 6b) the level of BAX and BCL-2 proteins in COLO 205 cells was not affected upon NaBt [5 mM] treatment. Lack of causal relationship between the p53 and NaBt activity was reported previously by Chopin et al. [46] and Kobayashi et al. [47], nonetheless, the extensive study are needed to clarify the involvement of p53 in NaBt-induced intrinsic apoptotic pathway.

Overall, NaBt-dependent proapoptotic effect has been correlated to its ability to modulate the expression of IAP family of antiapoptotic proteins. Kim et al. [31] showed

that in U87MG and A172 glioma cells overexpress survivin and XIAP proteins, which in turn attenuated TRAIL-dependent apoptosis. NaBt [5 mM] treatment was sufficient to down-regulate the expression of both proteins through inhibition of Cdc2 kinase activity [31]. One has to keep in mind, that XIAP and survivin-mediated apoptosis is not limited to extrinsic apoptotic pathway. Their respective overexpression could also efficiently block the mitochondria-associated cell death [48]. As shown on Fig. 6b, NaBt-induced [5 mM] intrinsic apoptosis was accompanied by the diminished XIAP and survivin levels and this effect was not reliant on caspases activation.

The expression of all anti-apoptotic proteins chosen for analyses is known to be regulated by distinct transcription factors, thus it is hard to identify direct target of NaBt action in COLO 205 cells. We suppose that observed NaBt-induced changes in the expression of anti- (cFLIP, BCL-x_L, XIAP, survivin) and pro-apoptotic (BAK) proteins could be explained by its HDACi characteristics. Even though, one has to bear in mind, that varied phenotypes of cancer cells and diverse cellular mediators of NaBt-induced apoptosis suggest that its effect is cell type specific and could not be explained by a common molecular mechanism.

Conclusion

Our results suggest that NaBt may serve as a good candidate for colon cancer therapy. NaBt is able to potentiate TNF-α-induced apoptosis in COLO 205 cells by eliminating the antiapoptotic protein (cFLIP) with concomitant overexpression of TNF-R1 protein. Moreover, NaBt treatment activates intrinsic apoptotic pathway irrespective to TNF-α treatment. It is believed that inhibition of the gene expression by NaBt would not affect normal cells. Our data suggests that NaBt should be seriously considered as an alternative adjuvant in anti-cancer strategy.

Acknowledgments We acknowledge Dr. Janusz Skierski (Flow Cytometry Laboratory, National Institute of Public Health, Warsaw, Poland) for his help in flow cytometry analysis. Support for this work was provided by grants No. N312 012 32/0761 and N N404 152 434 from the Ministry of Science and Higher Education in Poland.

References

1. Moss SF, Scholes JV, Holt PR (1996) Abnormalities of epithelial apoptosis in multistep colorectal neoplasia demonstrated by terminal deoxyuridine nick end labeling. Dig Dis Sci 41:2238–2247. doi:10.1007/BF02071407
2. Young GP, Gibson PR (1995) Butyrate and the human cancer cell. In: Cummins JH, Rombeau J, Sakata T (eds) Physiological and clinical aspects of short-chain fatty acids. Cambridge University Press, Cambridge, pp 319–336
3. Avivi-Green C, Polak-Charcon S, Madar Z, Schwartz B (2000) Apoptosis cascade proteins are regulated in vivo by high intracolonic butyrate concentration: correlation with colon cancer inhibition. Oncol Res 12:83–95
4. Earel JK, Van Oosten RL, Griffith TS (2006) Histone deacetylase inhibitors modulate the sensitivity of tumor necrosis factor-related apoptosis-inducing ligand-resistant bladder tumor cells. Cancer Res 66:499–507. doi:10.1158/0008-5472.CAN-05-3017
5. Liu CX, Zhang SZ, Zhang XW, Geng XL, Li TJ, Huang LH, Wang B (2005) Inhibitory effect of sodium butyrate on 1,2-dimethylhydrazine-induced tumorigenesis of colorectal cancer in mice. Ai Zheng 24:930–934
6. Cummings JH, Pomare EW, Branch WJ, Naylor CP, Macfarlane GT (1987) Short chain fatty acids in human large intestine, portal, hepatic and venous blood. Gut 28:1221–1227. doi:10.1136/gut.28.10.1221
7. Heerdt BG, Houston MA, Augenlicht LH (1997) Short-chain fatty acid-initiated cell cycle arrest and apoptosis of colonic epithelial cells is linked to mitochondrial functions. Cell Growth Differ 8:523–532
8. Pajak B, Orzechowski A, Gajkowska B (2007) Molecular basis of sodium butyrate-dependent proapoptotic activity in cancer cells. Adv Med Sci 52:83–88
9. Sealy L, Chalkley R (1978) The effect of sodium butyrate on histone modification. Cell 14:115–121. doi:10.1016/0092-8674(78)90306-9
10. Kruh J (1982) Effects of sodium butyrate, a new pharmacological agent, on cells in culture. Mol Cell Biochem 42:65–82
11. Nagata S (1997) Apoptosis by death factor. Cell 88:355–365. doi:10.1016/S0092-8674(00)81874-7
12. Schulze-Osthoff K, Ferrari D, Los M, Wesselborg S, Peter ME (1998) Apoptosis signaling by death receptors. Eur J Biochem 254:439–459. doi:10.1046/j.1432-1327.1998.2540439.x
13. Pajak B, Gajkowska B, Orzechowski A (2005) Cycloheximide-mediated sensitization to TNF-α-induced apoptosis in human colorectal cancer cell line COLO 205; role of FLIP and metabolic inhibitors. J Physiol Pharmacol 56(suppl 3):101–118
14. Hernandez A, Wang QD, Schwartz SA, Evers BM (2001) Sensitization of human colon cancer cells to TRAIL-mediated apoptosis. J Gastrointest Surg 5:56–65. doi:10.1016/S1091-255X(01)80014-7
15. Lippa MS, Srockbine LD, Le TT, Branstetter DG, Strathdee CA, Holland PM (2007) Expression of anti-apoptotic factors modulates Apo2L/TRAIL resistance in colon carcinoma cells. Apoptosis 12:1465–1478. doi:10.1007/s10495-007-0076-6
16. Natoni F, Diolordi L, Santoni C, Gilardini Montani G (2005) Sodium butyrate sensitizes human pancreatic cancer cells to both the intrinsic and the extrinsic apoptotic pathways. Biochim Biophys Acta 1745:318–329
17. Deveraux QL, Reed JC (1999) IAP family proteins suppressors of apoptosis. Genes Dev 13:239–252. doi:10.1101/gad.13.3.239
18. Jacobson MD, Burne JF, Raff MC (1994) Programmed cell death and Bcl-2 protection in the absence of a nucleus. EMBO J 13:1899–1910
19. McKeague AL, Wilson DJ, Nelson J (2003) Staurosporine-induced apoptosis and hydrogen peroxide-induced necrosis in two human breast cell lines. Br J Cancer 88:125–131. doi:10.1038/sj.bjc.6600675
20. Bradford MM (1976) A rapid and sensitive method for the quantitation of microgram quantities of protein utilizing the principle of protein-dye binding. Anal Biochem 72:248–254. doi:10.1016/0003-2697(76)90527-3
21. Watts AD, Hunt NH, Madigan MC, Chaudhri G (1999) Soluble TNF-alpha receptors bind and neutralize over-expressed transmembrane TNF-alpha on macrophages, but do not inhibit its processing. J Leukoc Biol 66:1005–1013

22. Pajak B, Turowska A, Orzechowski A, Gajkowska B (2008) Bisindolylmaleimide IX facilitates extrinsic and initiates intrinsic apoptosis in TNF-α-resistant human colon adenocarcinoma COLO 205 cells. Apoptosis 13:509–522. doi:10.1007/s10495-008-0194-9
23. Clem RJ, Cheng EHY, Karp CL, Kirsch DG, Ueno K, Takahashi A, Kastan MB, Griffin DE, Earnshaw WC, Veliuona MA, Hardwick JM (1998) Modulation of cell death by Bcl-xL through caspase interaction. Proc Natl Acad Sci USA 95:554–559. doi:10.1073/pnas.95.2.554
24. Johnson DE, Gastman BR, Wieckowski E, Wang GQ, Amoscato A, Delach SM, Rabinowich H (2000) Inhibitor of apoptosis protein hILP undergoes caspase-mediated cleavage during T lymphocyte apoptosis. Cancer Res 60:1818–1823
25. El Deiry WS (2001) Insights into cancer therapeutic design based on p53 and TRAIL receptor signaling. Cell Death Differ 8:1066–1075. doi:10.1038/sj.cdd.4400943
26. Ashkenazi A (2002) Targeting death and decoy receptors of the tumor-necrosis factor superfamily. Nat Rev Cancer 2:420–430. doi:10.1038/nrc821
27. Pajak B, Orzechowski A (2007) Sodium butyrate-dependent sensitization of human colon adenocarcinoma COLO 205 cells to TNF-α-induced apoptosis. J Physiol Pharmacol 58(suppl 3):163–176
28. Micheau O, Solary E, Hammann A, Dimanche-Boitrel MT (1999) Fas-ligand-independent, FADD-mediated activation of the Fas death pathway by anticancer drugs. J Biol Chem 274:7987–7992. doi:10.1074/jbc.274.12.7987
29. Chopin V, Slomianny C, Hondermarck H, Le Bourhis X (2004) Synergistic induction of apoptosis in breast cancer cells by co-treatment with butyrate and TNF-alpha, TRAIL, or anti-Fas agonist antibody involves enhancement of death receptors' signaling and requires P21(waf1). Exp Cell Res 298:560–573. doi:10.1016/j.yexcr.2004.04.038
30. Nakata S, Yoshida T, Horinaka M, Shiraishi T, Wakada M, Sakai T (2004) Histone deacetylase inhibitors upregulate death receptor 5/TRAIL-R2 and sensitize apoptosis induced by TRAIL/APO2-L in human malignant tumor cells. Oncogene 23:6261–6271. doi:10.1038/sj.onc.1207830
31. Kim EH, Kim HS, Kim SU, Noh EJ, Lee JS, Choi KS (2005) Sodium butyrate sensitizes human glioma cells to TRAIL-mediated apoptosis through inhibition of Cdc2 and the subsequent downregulation of survivin and XIAP. Oncogene 24:6877–6889. doi:10.1038/sj.onc.1208851
32. Pajak B, Orzechowski A (2007) IFN-α competes with TNF-α for STAT-1α—molecular basis for immune escape of human colon adenocarcinoma COLO 205 cells. Oncol Rep 18:1039–1045
33. Henshall DC, Bonislawski DP, Skradski SL, Lan JQ, Meller R, Simon RP (2001) Cleavage of bid may amplify caspase-8-induced neuronal death following focally evoked limbic seizures. Neurobiol Dis 8:568–580. doi:10.1006/nbdi.2001.0415
34. Kim R (2005) Recent advances in understanding the cell death pathways activated by anticancer therapy. Cancer 103:1551–1560. doi:10.1002/cncr.20947
35. Godefroy N, Lemaire C, Renaud F, Rincheval V, Perez S, Parvu-Ferecatu I, Mignotte B, Vayssiere JL (2004) p53 can promote mitochondria- and caspase-independent apoptosis. Cell Death Differ 11:785–787. doi:10.1038/sj.cdd.4401398
36. Wolf BB, Goldstein JC, Stennicke HR, Beere H, Amarante-Mendes GP, Salvesen GS, Green DR (1999) Calpain functions in a caspase-independent manner to promote apoptosis-like events during platelet activation. Blood 94:1683–1692
37. Zhang C, Baffi J, Cousins SW, Csaky KG (2003) Oxidant-induced cell death in retinal pigment epithelium cells mediated through the release of apoptosis-inducing factor. J Cell Sci 116:1915–1923. doi:10.1242/jcs.00390
38. Wu ZQ, Zhang R, Connie C, Zhang JF, Zhang YQ (2007) Histone deacetylase inhibitor-trichostatin A induced caspase-independent apoptosis in human gastric cancer cells. Chin Med J 120:2112–2118
39. Ruemmele FM, Schwartz S, Seidman EG, Dionne S, Levy E, Lentze MJ (2003) Butyrate induced Caco-2 cell apoptosis is mediated via the mitochondrial pathway. Gut 52:94–100. doi:10.1136/gut.52.1.94
40. Shimizu S, Narita M, Tsujimoto Y (1999) Bcl-2 family proteins regulate the release of apoptogenic cytochrome *c* by the mitochondrial channel VDAC. Nature 399:483–487. doi:10.1038/20959
41. Ruffolo SC, Shore GC (2003) Bcl-2 selectively interacts with the BID-induced open conformer of Bak, inhibiting Bak auto-oligomerization. J Biol Chem 278:25039–25045. doi:10.1074/jbc.M302930200
42. Basu A, Haldar S (1998) The relationship between Bcl2, Bax and p52: consequences for cell cycle progression and cell death. Mol Hum Reprod 4:1099–1109. doi:10.1093/molehr/4.12.1099
43. Gu W, Roeder RG (1997) Activation of p53 sequence-specific DNA binding by acetylation of the p53 C-terminal domain. Cell 90:595–606. doi:10.1016/S0092-8674(00)80521-8
44. Sakaguchi K, Herrera JE, Saito S, Miki T, Austin M, Vassilev A, Anderson CW, Apella E (1998) DNA damage activates p53 through a phosphorylation–acetylation cascade. Genes Dev 12:2831–2841. doi:10.1101/gad.12.18.2831
45. Juan LJ, Shia WJ, Chen MH, Yang WM, Seto E, Lin YS, Wu CW (2000) Histone deacetylase specifically down-regulate p53-dependent gene activation. J Biol Chem 275:20436–20443. doi:10.1074/jbc.M000202200
46. Chopin V, Toillon RA, Jouy N, Le Bourhis X (2002) Sodium butyrate induces p53-independent, Fas-mediated apoptosis in MCF-7 human breast cancer cells. Br J Pharmacol 135:79–86. doi:10.1038/sj.bjp.0704456
47. Kobayashi H, Tan EM, Fleming SE (2003) Sodium butyrate inhibits cell growth and stimulates p21WAF1/CIP1 protein in human colonic adenocarcinoma cells independently of p53 status. Nutr Cancer 46:202–211. doi:10.1207/S15327914NC4602_14
48. Che XF, Zheng CL, Owatari S, Mutoh M, Gotanda T, Jeung HC, Furukawa T, Ikeda R, Yamamoto M, Haraguchi M, Arima N, Akiyama S (2006) Overexpression of survivin in primary ATL and sodium arsenite induces apoptosis by down-regulating survivin expression in ATL cell lines. Blood 107:4880–4887. doi:10.1182/blood-2005-08-3423